Design and Control of a Compact, Modular Robot for Transbronchial Lung Biopsy

Stephanie Amack[1,*], **Margaret Rox**[1], **Jason Mitchell**[1], **Tayfun Efe Ertop**[1], **Maxwell Emerson**[1], **Alan Kuntz**[2], **Fabien Maldonado**[3], **Jason Akulian**[4], **Joshua Gafford**[1], **Ron Alterovitz**[2], **Robert J. Webster III**[1]

[1]Mechanical Engineering, Vanderbilt University, Nashville, TN, USA

[2]Computer Science, University of North Carolina at Chapel Hill, NC, USA

[3]Interventional Pulmonology, Vanderbilt University Medical Center, Nashville, TN, USA

[4]Interventional Pulmonology, University of North Carolina at Chapel Hill, NC, USA

Abstract

Lung cancer is one of the most prevalent and deadly forms of cancer, claiming more than 154,000 lives in the USA per year. Accurate targeting and biopsy of pulmonary abnormalities is key for early diagnosis and successful treatment. Many cancerous lesions originate in the peripheral regions of the lung which are not directly accessible from the bronchial tree, thereby requiring percutaneous approaches to collect biopsies, which carry a higher risk of pneumothorax, hemorrhage, and death in extreme cases. In prior work, our group proposed a concept for accessing the peripheral lung through the airways, via a bronchscope deployed steerable needle. In this paper, we present a more compact, modular, multi-stage robot, designed to deploy a steerable needle through a standard flexible bronchoscope, to retrieve biopsies from lesions in the peripheral regions of the lung. The robot has several stages that can control a steerable biopsy needle, as well as concentric tubes, which act as an aiming conduit. The functionality of this robot is demonstrated via closed-loop lesion targeting in a CT scanner. The steerable needle is controlled using a previously proposed sliding mode controller, based on feedback from a magnetic tracker embedded in the steerable needle's tip. Towards developing a clinically viable platform, this system builds on prior work through its modular, compact form factor, and workflow-conscious design that provides precise homing and the ability to interchange tools as needed.

Keywords

Lung Cancer; Robotics; Bronchoscopy; Biopsy; Minimally-Invasive Surgery

1 INTRODUCTION

In the United States, more people die from lung cancer than any other form of cancer, with an estimated 154,000 new deaths in 2018.[1] Lung cancer has among the lowest 5-year

---

*:corresponding: author stephanie.r.amack@vanderbilt.edu.

survival rates of all the major cancers (18.2%[2]), and symptoms do not typically occur until the cancer is at an advanced stage.[1] As such, early detection is instrumental for mounting an effective, targeted oncologic treatment plan and eradicating the disease.

When a pulmonary abnormality is identified via computed tomography (CT) scans during a screening, acquiring representative tissue samples of this lesion through biopsy is paramount to obtaining a definitive diagnosis. The two most common approaches for acquiring biopsy samples are percutaneous (transthoracic) and bronchoscopic (transbronchial) approaches. During a percutaneous biopsy, a needle is inserted through the chest and into the lung under CT guidance, puncturing the pleural membrane in the process, and a tissue sample is cut or aspirated from the suspicious lesion for further histopathological analysis and etiological determination. Despite high sensitivity, specificity, and diagnostic yield for larger lesions,[3] trans-pleural access carries a substantial risk of intraoperative complications including pneumothorax (or lung collapse, which occurs in up to 26% of cases[4–6]), pulmonary bleeding (which occurs in up to 30% of cases[5]), and even occasional reports of embolism[7] and death.[8] In addition, diagnostic yield falls off substantially for lesions smaller than 10mm in diameter, due in part to technical difficulties associated with navigating to such a small lesion.[3,9]

In transbronchial approaches, a flexible bronchoscope is inserted into the body through the patient's mouth, and navigated through the bronchial passages towards the site of the lesion. Instruments such as a flexible aspiration needle, brush, or biopsy forceps are passed through the bronchoscope and used to collect several (4–6[10]) samples of the lesion.[11] While transbronchial biopsy is less traumatic than percutaneous biopsy, with lower complication rates (1–6% for pneumothorax, 1–2% for pulmonary bleeding[10]), its utility is limited to larger lesions located within or in close proximity to the bronchial tree,[12] and only in proximal segments where the bronchial diameter is large enough to accept the diameter of the bronchoscope. Therefore, despite reduced invasiveness and morbidity, the low diagnostic yield for small, peripheral lesions has limited the efficacy of transbronchial approaches.[13]

Commercial efforts towards enabling accurate peripheral lung biopsies transbronchially have primarily focused on imaging (Endobronchial Ultrasound (EBUS) bronchoscope from Olympus[14]), electromagnetic navigation (SuperDimension from MedTronic,[15] SPiN from Veran Medical[16]) and virtual navigation (Archimedes from Bronchus Medical[17]). More recently, flexible bronchoscopy robots have been released (Monarch system from Auris, Inc.) or are currently under development (Ion system from Intuitive Surgical, Inc.) with the goal of improving yield in transbronchial peripheral lesion biopsies through enhanced distal dexterity. However, while these platforms offer greater maneuverability in the airway to access smaller diameter bronchi and aim biopsy needles within the bronchus, they do not address steering the needle within the parenchyma to target remote lesions.

Recognizing the merits and drawbacks of percutaneous and bronchoscopic approaches, our group has previously proposed combining steerable needles with concentric tube robots to enable peripheral lesion access and biopsy through bronchoscopic delivery platforms.[18–20] In this approach, the idea is that the physician will first navigate a standard bronchoscope into the bronchus to the desired bronchial exit location, which may be manually selected by

the physician or indicated using planning software. A robotically controlled concentric tube stage is then deployed through the bronchoscope, which serves as an aiming conduit to aim the last stage, which consists of a bevel-tip steerable needle. A sliding-mode controller[21] is then used to guide the needle along a planned path to the peripheral lesion. This multi-stage robotic approach aims to combine the high diagnostic yield of percutaneous biopsy with the reduced invasiveness and morbidity of transbronchial approaches.

To date, a significant amount of work has gone into the foundational design, optimization, and validation of concentric tube robots in isolated, controlled, or benchtop environments[22–25] Similarly, significant work has been done on bevel tip design, optimization, and validation.[26–29] As mentioned previously, a preliminary multi-stage peripheral lung biopsy robot design was developed by Swaney et al.,[18,19] where the primary focus was on demonstrating feasibility of the multi-stage deployment concept. We build on this prior work by developing a new robotic actuation system that fits within the system paradigm of Swaney et al., and controls both concentric tubes and a bevel tip steerable needle using a modular, compact, and workflow-conscious design. This work complements related work in motion planning[20] toward a new paradigm of multi-stage concentric tube/ steerable needle robots for peripheral lung biopsy. In Section 2, we describe the design of the compact actuation unit. In Section 3, we present preliminary results of closed-loop lesion targeting experiments performed on a biological tissue analog. Finally, in Section 4, we summarize the results and discuss future work.

2 COMPACT ACTUATION UNIT DESIGN

We developed a compact actuation system to deliver and control the multi-stage transbronchial concentric tube/needle device. The actuation unit we describe in this paper, shown in Figure 1, features four carriages, each with the ability to control the rotation and translation of the tools passed through them. Each carriage is functionally identical, and the system can accept arbitrary configurations of tools. For example, in a multi-stage configuration for lesion targeting, one carriage is used to advance and rotate the steerable needle, one carriage is used to advance and rotate the concentric tube for positioning the steerable needle and aiming the workspace, and two are left over for other functions (i.e. additional concentric tubes). Motors for actuating each degree of freedom are outfitted with planetary gearsets and optical encoders, and are mounted onto the proximal end of the system. Motion is transmitted to each tool via a leadscrew (which translates the tool carriage on low-friction linear guiderails) and a geared square shaft (which engages with a spur gear attached to the tool for rotation). The high-stiffness chassis is machined from aluminum, and the entire system can be mounted onto a lockable arm (Noga Engineering, Israel) for passive positioning prior to or during the procedure.

2.1 Tool Quick-Connect

The ability to rapidly and easily interchange various tools as desired is an important capability of this system that has not been realized in prior bevel tip steerable needle systems. This modularity can be exploited to configure the system in a way that is optimal for the particular lesion being targeted, as additional modules (e.g. additional concentric

tubes) can be added to increase dexterity as needed. Each tool is pre-configured with an attached spur gear, and can be quickly inserted into or removed from its carriage. The mechanism, shown in Figure 2, features two spring-loaded levers which deflect to accept the spur gear hub, and retract to couple the gear hub between two rolling elements (one on each lever) and the mating gear mounted on the carriage. The spur gear on the tool meshes with the central mating gear on the carriage, enabling the transmission of rotational motion from the square shaft. The spring tension between the levers can be adjusted, thereby adjusting the preload between the tool gear and the mating carriage gear, to minimize backlash.

2.2 Sensor-Based Homing of Actuated Degrees of Freedom

Since high resolution motor encoders are typically incremental, an initialization routine is necessary for the robot to know precisely where each carriage (and hence each tube's home position) is in both linear insertion and axial rotation degrees of freedom. Our system's encoders provide a linear resolution of 0.021 μm and an angular resolution of 0.0021°. We designed a precise, systematic homing protocol to establish a repeatable home position for all degrees of freedom of the robot. Optical photointerruptors (OPB625, TT Electronics) are responsible for translational homing, and are built into the stationary chassis of the actuation unit, one for each carriage. These trigger when a protrusion on the carriage breaks the optical path of the sensor. Rotational reflective sensors (OPB608V Reflective Sensor, TT Electronics) are placed on plastic support arms mounted to the chassis so that they align with the gear hub when the translational sensor is triggered (Figure 3), and a reflective homing mark on the gear hub indicates the rotational home position. The homing protocol, which initiates upon system power-up, is carried out as follows: (1) each carrier is retracted until the chassis-mounted translational sensor associated with that carriage is activated, establishing a home position on the linear axis, (2) the rotational degree of freedom is advanced unidirectionally until the chassis-mounted rotational sensor is triggered (Figure 3(right)), thereby establishing home position on the rotational axis. To quantify the accuracy of the homing protocol, we conducted 12 repeatability tests on each axis. Homing precision was measured to have a standard deviation of ±7.3 μm (maximum difference 25.3 μm) and ±0.09°(maximum difference 1.67°), respectively.

3 EXPERIMENTAL RESULTS

Ultimately, the compact actuation system described in the previous section will be used to deploy a steerable needle, and one or more concentric tubes used to aim it, through a bronchoscope port with the goal of enabling accurate and safe access to peripheral lung lesions. Such a system will likely use electromagnetic tracking combined with imaging information to accurately steer through lung tissue to the physician's desired target. We have previously demonstrated steering to targets using a rapid replanning framework[30] and via sliding mode control.[21] To demonstrate the capabilities of our new actuation unit we performed the following experiments using the sliding mode controller to deliver it to desired target points selected in CT images.

The experimental setup is shown in Figure 4. The sliding mode controller described by Rucker et al.[21] was implemented via the Robot Operating System (ROS). We used this

system to target lesions embedded in phantom tissue made from synthetic ballistics gel (Humimic Medical, Fort Smith, AR). A 0.41mm diameter, 5-DOF magnetic tracking coil (Northern Digital Inc., Canada) was embedded in the steerable needle tip. The 6th degree of freedom (rotation about the needle axis) was inferred from needle base angle. The shaft of the steerable needle used in these experiments was made from a 0.57mm outer diameter nitinol tube. The tip (in which the tracking coil was embedded) was made from a short length of 0.80 mm nitinol tube with a flexure hinge and a 10° bevel tip, as described by Swaney.[29]

3.1   Closed-Loop Needle Steering: Benchtop Experiments

The closed-loop targeting performance of the system was verified in the ballistics gel phantom mentioned previously. This experiment was done on the benchtop in the lab with magnetic tracker feedback. Eight different target points within the steerable needle's workspace were selected, and the needle was steered to each using the sliding mode controller. As shown in Figure 5, the controller was able to steer the needle to the target points successfully. The mean error between final needle tip positions and target points was 0.46 mm ±0.28 mm (maximum 0.96 mm).

3.2   Closed-Loop Needle Steering: In CT Scanner Experiments

In this set of experiments, we tested the ability of the system to hit targets identified in CT images. Spherical objects simulating lung lesions were embedded in the ballistics gel phantom. The phantom was scanned using a CT scanner (Xoran Technologies, USA) to determine the location of these lesions in CT space. Twelve fiducial markers were attached to the phantom (as shown in the inset in Figure 4) to register CT space to magnetic tracker space. The locations of the CT space lesion targets were transformed into magnetic tracker space, the steerable needle was steered to hit these targets using magnetic tracker feedback (just as in the benchtop experiments above), and the final error was assessed using a post-insertion CT scan. Four simulated lesions were targeted as shown in Figure 6, and all were hit successfully with the needle. The paths followed by the needle to each lesion are shown in Figure 6(b). The needle path and lesions segmented from the postoperative CT images are shown in Figure 6(c) for one of the lesions targeted. Since the target lesions used in these experiments were hard compared to the surrounding tissue, we did not attempt to push the needle tip inside them, to avoid damaging the tip, instead stopping the needle at the surface of the lesion. Based on this, we confirmed that the needles hit each desired lesion, but did not compute a final tip accuracy in CT space. These results illustrate that the robotic system is able to accurately target lesions identified in CT images.

4.   CONCLUSION

In this work, we have presented a new modular, compact, multi-stage robot for transbronchial biopsy of peripheral lung lesions. The ability to quickly connect and disconnect needles and concentric tubes aids in the usability of the system and will be an important capability in the clinical translation of this technique. Integration of homing capabilities to precisely initialize tool positions enables repeatable experiments, and rapid tool interchange. Closed-loop control experiments in phantom tissue demonstrated that this

new robot can effectively steer a bevel tip needle in phantom tissue. Future work will focus on the integration of concentric tube stages and experiments through a bronchoscope, which we expect will require integrating a model for torsional needle dynamics[31] or an observer-based approach[32] to extract the needle's roll degree of freedom. Before clinical translation, we must also address sterility considerations and validate the system in vivo in an animal model. Thus, while there remains much work to be done, the results presented in this paper take important steps toward the ultimate goal of a practical clinical system for transbronchoscopic needle steering, enabling rapid tool changes and homing capabilities in such a system for the first time.

REFERENCES

[1]. American Cancer Society, "Cancer Facts and Figures 2018," tech. rep. (2018).

[2]. U.S. Cancer Statistics Working Group, "U.s. cancer statistics data visualizations tool, based on november 2017 submission data (1999–2015): U.s. department of health and human services," Centers for Disease Control and Prevention and National Cancer Institute (2018).

[3]. Winokur RS, Pua BB, Sullivan B, and Madoff DC, "Percutaneous lung biopsy: Technique, efficacy, and complications," Seminars in Interventional Radiology 30(2), 121–127 (2013). [PubMed: 24436527]

[4]. Wang Memoli JS, Nietert PJ, and Silvestri GA, "Meta-analysis of guided bronchoscopy for the evaluation of the pulmonary nodule," Chest 142(2), 385–393 (2012). [PubMed: 21980059]

[5]. Yeow KM, Su IH, Pan KT, Tsay PK, Lui KW, Cheung YC, and Chou ASB, "Risk factors of pneumothorax and bleeding: Multivariate analysis of 660 CT-guided coaxial cutting needle lung biopsies," Chest 126(3), 748–754 (2004). [PubMed: 15364752]

[6]. Saji H, Nakamura H, Tsuchida T, Tsuboi M, Kawate N, Konaka C, and Kato H, "The incidence and the risk of pneumothorax and chest tube placement after percutaneous CT-guided lung biopsy: The angle of the needle trajectory is a novel predictor," Chest 121(5), 1521–1526 (2002). [PubMed: 12006438]

[7]. Fiore L, Frenk NE, Martins GLP, Viana PCC, and de Menezes MR, "Systemic Air Embolism after Percutaneous Lung Biopsy: A Manageable Complication," Journal of Radiology Case Reports 11(6), 6–14 (2017). [PubMed: 29299093]

[8]. Lorenz J and Blum M, "Complications of percutaneous chest biopsy," Seminars in Interventional Radiology 23(2), 188–193 (2006). [PubMed: 21326762]

[9]. Kothary N, Lock L, Sze DY, and Hofmann LV, "Computed tomography-guided percutaneous needle biopsy of pulmonary nodules: Impact of nodule size on diagnostic accuracy," Clinical Lung Cancer 10(5), 360–363 (2009). [PubMed: 19808195]

[10]. Jain P, Hadique S, and Mehta A, "Transbronchial Lung Biopsy," in [Interventional Bronchoscopy: A Clinical Guide], 10, 15–44 (2013).

[11]. Shure D, "Transbronchial biopsy and needle aspiration," Chest 95(5), 1130–1138 (1989). [PubMed: 2651036]

[12]. Baaklini WA, Reinoso MA, Gorin AB, Sharafkaneh A, and Manian P, "Diagnostic yield of fiberoptic bronchoscopy in evaluating solitary pulmonary nodules," Chest 117(4), 1049–1054 (2000). [PubMed: 10767238]

[13]. Gasparini S, Bonifazi M, and Wang KP, "Transbronchial needle aspirations vs. percutaneous needle aspirations," Journal of Thoracic Disease 7(1), 300–303 (2015).

[14]. Herth FJ, Ernst A, Eberhardt R, Vilmann P, Dienemann H, and Krasnik M, "Endobronchial ultrasound-guided transbronchial needle aspiration of lymph nodes in the radiologically normal mediastinum," European Respiratory Journal 28(5), 910–914 (2006).

[15]. Khandhar SJ, Bowling MR, Flandes J, Gildea TR, Hood KL, Krimsky WS, Minnich DJ, Murgu SD, Pritchett M, Toloza EM, Wahidi MM, Wolvers JJ, and Folch EE, "Electromagnetic navigation bronchoscopy to access lung lesions in 1,000 subjects: First results of the prospective,

multicenter NAVIGATE study," BMC Pulmonary Medicine 17(1), 1–9 (2017). [PubMed: 28049457]

[16]. Gilbert C, Akulian J, Ortiz R, Lee H, and Yarmus L, "Novel bronchoscopic strategies for the diagnosis of peripheral lung lesions: Present techniques and future directions," Respirology 19(5), 636–644 (2014). [PubMed: 24797257]

[17]. Herth FJ, Eberhardt R, Sterman D, Silvestri GA, Hoffmann H, and Shah PL, "Bronchoscopic transparenchymal nodule access (BTPNA): First in human trial of a novel procedure for sampling solitary pulmonary nodules," Thorax 70(4), 326–332 (2015). [PubMed: 25746631]

[18]. Swaney PJ, Mahoney AW, Remirez AA, Lamers E, Hartley BI, Feins RH, Alterovitz R, and Webster RJ, "Tendons, concentric tubes, and a bevel tip: Three steerable robots in one transoral lung access system," Proceedings - IEEE International Conference on Robotics and Automation, 5378–5383 (2015).

[19]. Swaney PJ, Mahoney AW, Hartley BI, Remirez AA, Lamers E, Feins RH, Alterovitz R, and Webster RJ, "Toward Transoral Peripheral Lung Access: Combining Continuum Robots and Steerable Needles," Journal of Medical Robotics Research 02(01), 1750001 (2017).

[20]. Kuntz A, Torres LG, Feins RH, Webster RJ, and Alterovitz R, "Motion planning for a three-stage multilumen transoral lung access system," IEEE International Conference on Intelligent Robots and Systems, 3255–3261 (2015).

[21]. Rucker DC, Das J, Gilbert HB, Swaney PJ, Miga MI, Sarkar N, and Webster RJ III, "Sliding Mode Control of Steerable Needles," IEEE Transactions on Robotics 29(5), 1289–1299 (2013). [PubMed: 25400527]

[22]. Mahoney AW, Gilbert HB, and W. RJ III, [A Review of Concentric Tube Robots: Modeling, Control, Design, Planning, and Sensing], ch. 7, 181–202.

[23]. Burgner-Kahrs J, Rucker DC, and Choset H, "Continuum Robots for Medical Applications: A Survey," IEEE Transactions on Robotics 31(6), 1261–1280 (2015).

[24]. Dupont PE, Lock J, Itkowitz B, and Butler E, "Design and control of concentric-tube robots," IEEE Transactions on Robotics 26(2), 209–225 (2010). [PubMed: 21258648]

[25]. Rucker DC, Jones BA, and Webster III RJ, "A geometrically exact model for externally loaded concentric-tube continuum robots," IEEE Transactions on Robotics 26(5), 769 (2010). [PubMed: 21566688]

[26]. Swaney PJ, Burgner J, Gilbert HB, and Webster III RJ, "A Flexure-Based Steerable Needle: High Curvature with Reduced Tissue Damage," IEEE Transactions on Biomedical Engineering 60(4), 906–909 (2013). [PubMed: 23204267]

[27]. Scali M, Pusch TP, Breedveld P, and Dodou D, "Needle-like instruments for steering through solid organs: A review of the scientific and patent literature," Proceedings of the Institution of Mechanical Engineers, Part H: Journal of Engineering in Medicine 231(3), 250–265 (2017).

[28]. Adebar TK, Greer JD, Laeseke PF, Hwang GL, and Okamura AM, "Methods for improving the curvature of steerable needles in biological tissue," IEEE Transactions on Biomedical Engineering 63(6), 1167–1177 (2016). [PubMed: 26441438]

[29]. Swaney PJ, Design and Modeling of Distal Dexterity Mechanisms for Needle-sized Robots: Systems for Lung and Endonasal Interventions, PhD thesis, Vanderbilt University (2016).

[30]. Patil S, Burgner J, Webster RJ, and Alterovitz R, "Needle steering in 3-d via rapid replanning," IEEE Transactions on Robotics 30(4), 853–864 (2014). [PubMed: 25435829]

[31]. Swensen JP, Lin M, Okamura AM, and Cowan NJ, "Torsional dynamics of steerable needles: modeling and fluoroscopic guidance," IEEE Transactions on Biomedical Engineering 61(11), 2707–2717 (2014). [PubMed: 24860026]

[32]. Kallem V and Cowan NJ, "Image guidance of flexible tip-steerable needles," IEEE Transactions on Robotics 25(1), 191–196 (2009). [PubMed: 20431694]
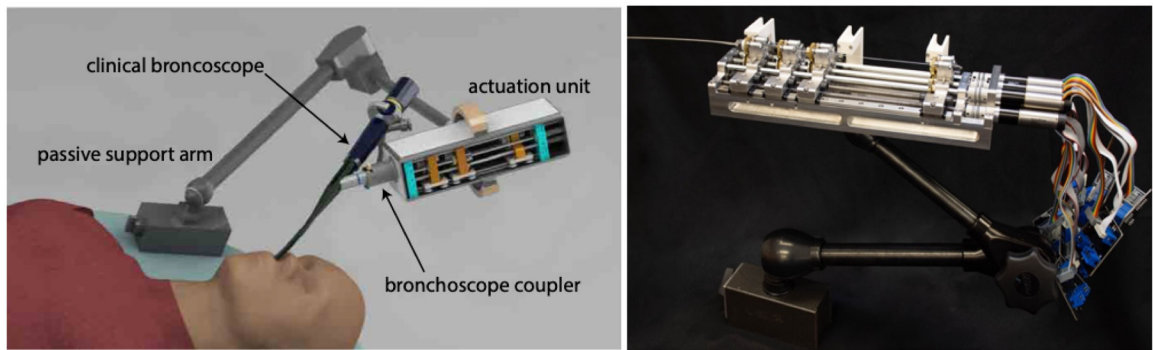
Figure 1.
Compact actuation system for transbronchial lung biopsy robot: *(left)* system rendering, *(right)* fabricated actuation unit held by Noga arm.
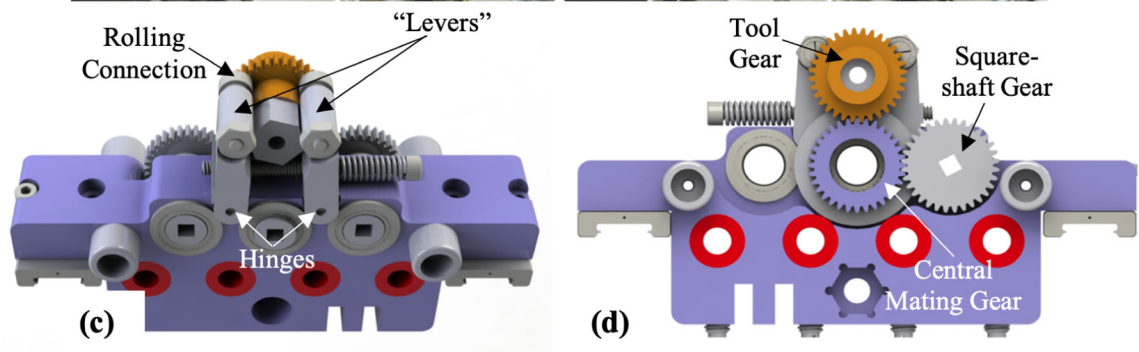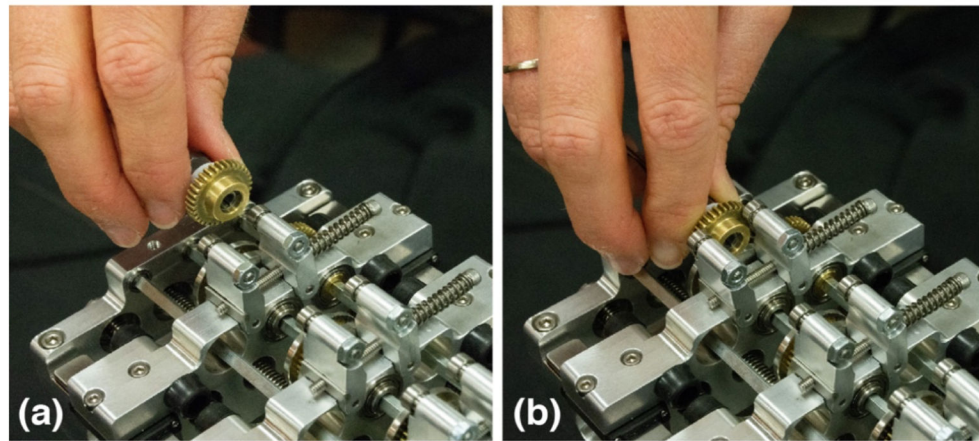
Figure 2.
Tool quick-connect mechanism: *(a)* before and *(b)* after the tool gear is inserted. *(c)* CAD rendering of the top view of the lever mechanism with *(d)* showing gear engagement.
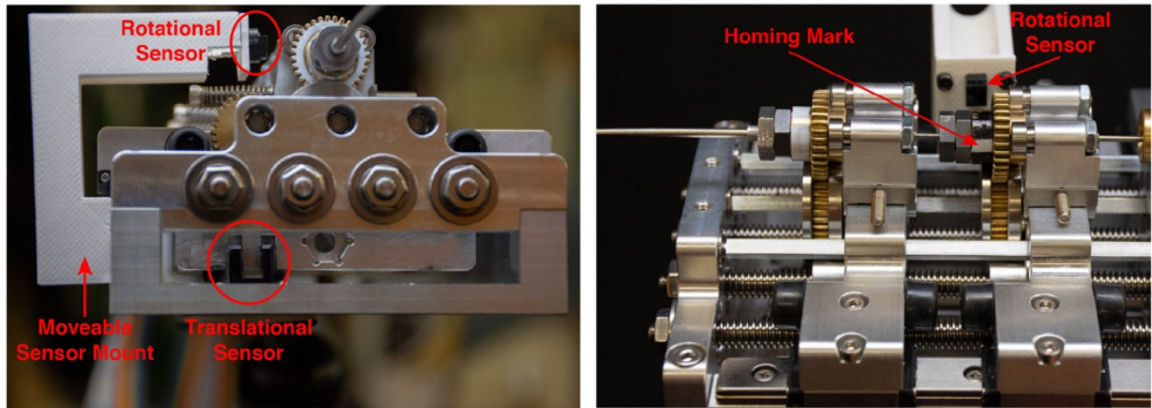
Figure 3.
Homing sensors: *(left)* front view of the actuation unit showing the placement of the rotational and translational sensors, *(right)* side view of the actuation unit showing the reflective fiducial.
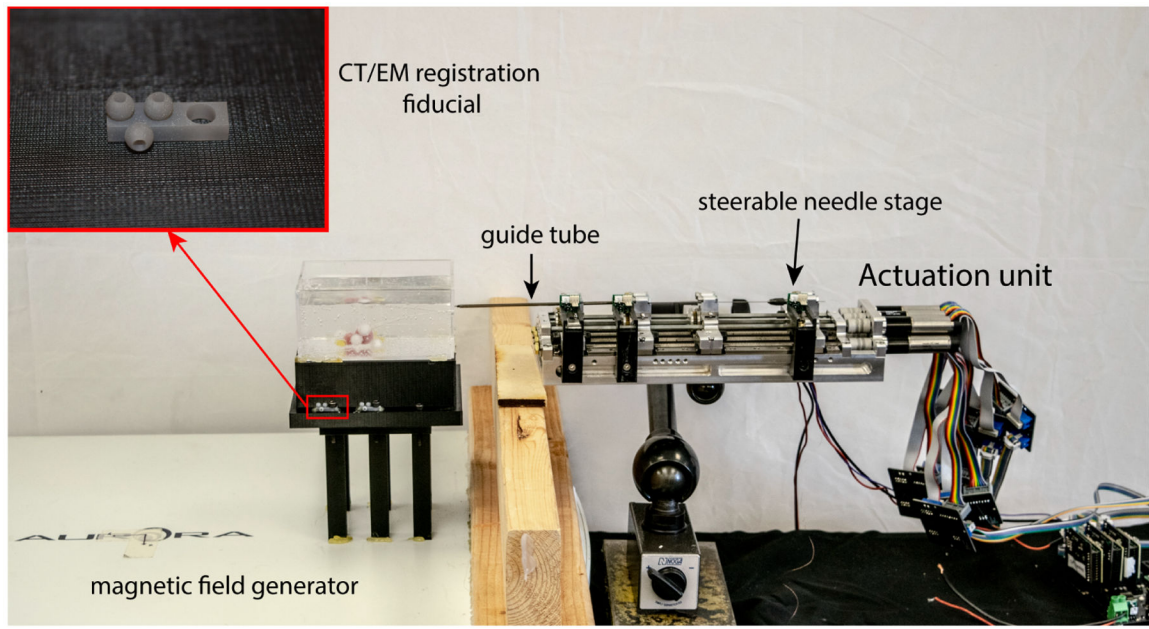
Figure 4.
Experimental setup for closed-loop needle steering and lesion targeting, where the inset shows an enlarged view of the fiducial markers.
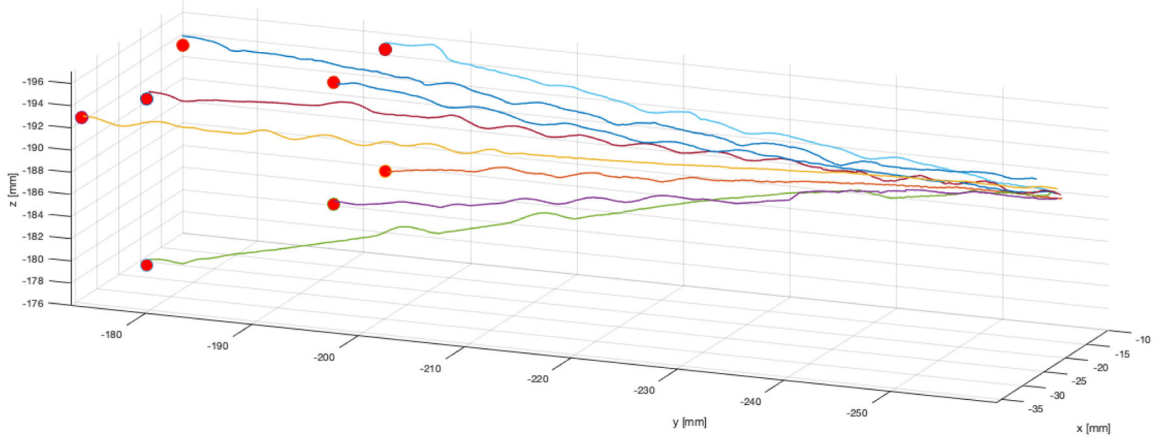
Figure 5.
Benchtop needle steering experimental needle tip paths, as measured by the magnetic tracker embedded in the needle's tip. The target points selected in magnetic tracker space are indicated by red spheres. Data points in the traces above are spaced approximately 78μm from one another, and 25-point moving average was used to filter sensor noise prior to plotting. The slight wobbles in the traces indicate times when the closed loop controller re-oriented the flexure-tip needle (the tip of the bevel is plotted).
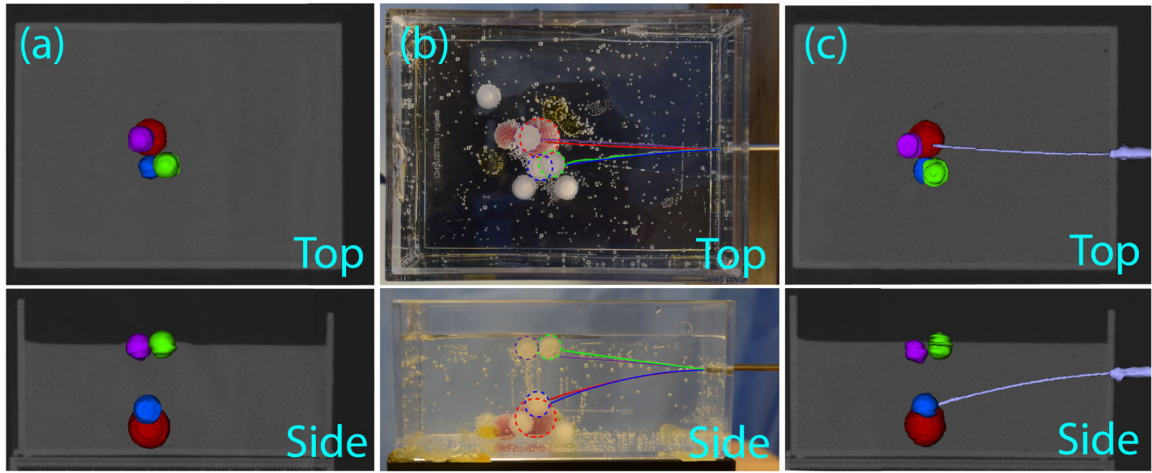
Figure 6.
Experimental results for the lesions targeted from pre-operative CT scan: *(a)* top and side views of the reconstructed pre-operative CT scan of the phantom with the four target lesions segmented: 9.5mm diameter plastic spheres are shown in purple, blue, and green, and a 13mm diameter silicon sphere is shown in red, *(b)* top and side views of the needle tip trajectories shown in the phantom, where each trajectory is indicated by the color of its corresponding target lesion, *(c)* an example post-operative reconstructed CT image displaying the needle successfully reaching the far red lesion.